Does Water Play a Crucial Role in the Growth of ZnO Nanoclusters in ZnO/Cu Catalyst?

Saptarshi Ghosh Dastider,[†,‡] Abhishek Ramachandra Panigrahi,[†,¶] Arup Banerjee,[§,‖] Krishna Kanta Haldar,[‡] Alessandro Fortunelli,[⊥] and Krishnakanta Mondal[*,†]

†*Department of Physics, Central University of Punjab, Bathinda, India-151401*

‡*Department of Chemistry, Central University of Punjab, Bathinda, India-151401*

¶*Department of Zoology, Central University of Punjab, Bathinda, India-151401*

§*Human Resources Development Section, Raja Ramanna Centre for Advanced Technology, Indore 452013, India*

‖*Homi Bhabha National Institute, Training School Complex, Anushaktinagar, Mumbai 400094, India*

⊥*CNR-ICCOM, Consiglio Nazionale delle Ricerche, ThC2-Lab, Pisa 56124, Italy*

E-mail: krishnakanta1987@gmail.com

Abstract

Catalytically active configuration of ZnO/Cu in the commercial $ZnO/Cu/Al_2O_3$ catalyst for methanol synthesis from CO_2 is still not clear. In this study, we employ density functional theory based methods to shed light on the structure and stoichiometry of ZnO clusters both free in the gas phase and also deposited on the Cu(111) surface under methanol synthesis conditions. Specifically, we investigate the structural evolution of ZnO clusters in presence of hydrogen and water. We find that the stability of ZnO clusters increases with the concentration of water till the ratio of Zn

and OH in the clusters reaches 1:2, with a morphological transition from planar to 3D configurations for clusters containing more than 4 Zn atoms. These clusters exhibit weak interaction with CO_2, and water is predicted to block the active center. The Cu(111) surface plays an important role in enhancing the adsorption of CO_2 on the ZnO/Cu(111) systems. We infer that ZnO nano-structures covered with OH species may be the morphology of the ZnO during the methanol synthesis from the hydrogenation of CO_2 on the industrial catalyst.

Introduction

Nano-structures of zinc oxide (ZnO) have attracted considerable attention of both theoreticians and experimentalists, due to their potential applications in optoelectronic devices, sensors, display devices and catalysis.[1–9] In particular, recently, the catalytic property of ZnO nano-structures have widely been investigated for many important reactions notably, waste water treatment by water splitting[10–15] and large scale production of methanol from the gas mixture of $CO_2/CO/H_2$.[5,6,16–21] For the industrial scale of methanol synthesis, it is reported that ZnO nano-structures in combination with Cu nano-particles supported on Al_2O_3 serve as the reaction centre.[5,16–18] A large number of investigations have been carried out on ZnO/Cu systems to understand the morphology of ZnO in the industrial catalyst $ZnO/Cu/Al_2O_3$.[22–27] However, the morphology and atomistic configuration of the ZnO nano-structures in contact with Cu is still not clear.[5,16] It is reported that the morphology of ZnO on Cu surface significantly gets altered during methanol synthesis from CO_2.[18,27,28] Lunkenbein et al showed that ZnO on Cu nano-particle exhibits phase change from rocksalt to wurtzite to graphetic film depending upon the reaction conditions during methanol synthesis.[16] In an another study, Wu et al observed that the water produced during methanol synthesis from CO_2 ($CO_2+3H_2 \rightarrow CH_3OH + H_2O$) accelerates the crystallization of Cu and ZnO in the catalyst.[29] This leads to to the deactivation of the catalyst.[29] On the other hand, Zachopoulos et al using thermodynamic analysis revealed that the in-situ water adsorption

during the hydrogenation of CO_2 may lead to 15% higher methanol production.[30] Therefore, the role of water in the hydrogenation of CO_2 towards methanol is under debate.

Very recently, it has been experimentlally shown that during methanol synthesis hydroxylated ZnO films or islands may exist at the interface of Cu and Al_2O_3 .[6,7] Similarly, our recent theoretical investigation showed that Cu supported ZnO nano-structures undergo a triangular reconstruction with composition of $Zn_6O_7H_7$ in presence of H_2 and H_2O and under methanol synthesis conditions. In this study, we consider graphitic film like structure of ZnO supported on Cu(111). However, to get a clear picture of the morphology of ZnO-Cu interface under industrial methanol synthesis condition which includes the presence of hydrogen and water we need to explore further considering different nano-structures of ZnO on Cu surface. Theoretically, the structural and electronic properties of $(ZnO)_n$, n=2-48, nano-clusters in the gas phase are extensively investigated in the literature.[31–33] However, a very few theoretical studies have reported the investigation of supported ZnO nano-structures[28] because such studies are computationally very expensive. Moreover, the effect of H_2 and H_2O on the structural, electronic and chemical properties of ZnO nano-clusters are not reported in the literature. Therefore, an extensive study on the properties of the free and supported ZnO nano-clusters in presence of H_2 and H_2O will be of interest. To minimize the computational cost, in the present work, first, we explore the possible configurations of $(ZnO)_n$ nanoclusters, where n=3 - 6, in presence of H_2 and H_2O. As a major result, we find that the ZnO clusters are fully hydroxylated under reaction conditions, i.e., they transform into $Zn(OH)_2$ species. We also highlight the evolution of structures from 2D to 3D as a function of size and of concentration of H_2O, and we unveil the relationship between 2D-¿3D transition and the formation of H2O adsorbed species. Further, the activity of the these clusters towards CO_2 adsorption of CO_2 molecule and activation is assessed. Finally, we investigate the effect of surface by considering these clusters supported Cu(111) surface on the adsorption and activation of CO_2 molecule at the ZnO-Cu interface.

Computational Method

In this work, we perform all the calculations using the DFT-based method as implemented in GPAW[34,35] and Gaussian09. The global minima of the clusters discussed in the present work are identified using basin hopping[36,37] (BH) method as implemented in ASE patched with GPAW. The details of method for finding the global minima is discussed in the supporting information. The global minima obtained from basin hopping method are further optimized using Gaussian09 with Becke's three parameter hybrid exchange functional.[38] For Zinc the larger basis set LanL2DZ[39] is used, for O and H Dunning's correlation consistent triple zeta basis set with added diffuse functions (AUG-cc-PVTZ)[40] is used. Geometry optimization process was done in g Gaussian09 with a force cut-off of $4.5 * 10^{-3}$ hartree/Bohr. The same method is used for the investigation of adsorption and activation of CO_2 on clusters in the gas phase.

For the study on the interaction of CO_2 with Cu(111) supported clusters we use the projector augmented wave approach, as implemented in GPAW, where the wave functions are represented on real space grids with grid spacing h = 0.18 for all the calculations. The exchange-correlation functional is approximated at GGA level using the formalism of Perdew, Burke, and Ernzerhof.[41] The FIRE algorithm[42] relaxes structures with a maximal force threshold of 0.05 eV. The Kohn-Sham eigenstates are occupied using a Fermi distribution with k_B T = 0.1 eV, and the total energies are extrapolated to T = 0 K.

Results and Discussions

To understand the effect of H and OH on the structural and electronic properties of the $(ZnO)_n$ clusters (where n=3-6), first, we identify the global minima of the hydrogenated and hydroxilated $(ZnO)_n$ clusters using basin hopping method. This method is discussed in Computational Details section. The initial geometries of the pure $(ZnO)_n$ clusters are taken from the literature.[33] These structures are re-optimized using the method discussed in

the previous section. We observe that all the $(ZnO)_n$ clusters possess symmetrical ring like structures, which are shown in Figure S1 of the supporting information (SI). In Table S2 we tabulate the average Zn-Zn and Zn-O bond lengths for all the ZnO clusters considered in the present work along already reported values. We find that the average Zn-Zn and Zn-O bond lengths reported in present work are in good agreement with the data available in the literature.[33] This indicates that the method adopted in the present work is suitable for the study of the systems based on ZnO. In the next section we carry out a discussion on the effect of hydrogen on the properties of ZnO clusters.

Hydrogenation of $(ZnO)_n$ Clusters

From our previous study[27] it is evident that the ZnO systems are more stable when all the oxygen atoms of ZnO are covered with hydrogen atoms. Keeping this in mind in the present study we consider fully hydrogenated ZnO clusters. The global minimum structures of these hydrogenated clusters are identified using the global minima search method discussed in Computational Details. The global minima of $(ZnOH)_n$, where n=3 - 6, clusters are shown in Figure 1. We observe a significant structural change in the ring-like geometries of the pure ZnO clusters due to the presence of hydrogen on these clusters. It can be seen from Figure 1 that the symmetrical ring-like ZnO structures convert into structures with branches with OH bridging. To quantify the structural change due to hydrogenation we compare Zn-Zn and Zn-O bond lengths of the pure ZnO clusters with those of the hydrogenated clusters. The corresponding results are compiled in Table S3. From this table we can see that the average Zn-Zn (Zn-O) bond length of hydrogenated clusters is approximately 3.27 (1.98) Å which is around 0.4 (0.2) Å larger than that of the ZnO clusters. These Zn-Zn and Zn-O bond lengths of hydrogenated clusters are found to be comparable to those of the bulk $Zn(OH)_2$ system(Zn-Zn = 3.2 Å Zn-O = 2.1 Å).

To understand the stability of the hydrogenated clusters we calculate the relative energies of these systems with respect to their corresponding pure clusters. The relative energies are

calculated using the equation

$$E_{rel} = E_{(ZnOH)_n} - E_{(ZnO)_n} - nE_H \tag{1}$$

where, $E_{(ZnOH)_n}$ and $E_{(ZnO)_n}$ are the energies of the hydrogenated and non-hydrogenated ZnO clusters, respectively and $E_H = \frac{1}{2}E_{H_2}$, E_{H_2} is the energy of a H_2 molecule, n is the number of hydrogen atoms present in the system. The relative energies of the $(ZnOH)_n$ clusters are compiled in the fifth column of Table S3. From this table we find that the hydrogenated clusters are more stable than that of the corresponding pristine ZnO clusters. In particular, it is found that the hydrogenated structures are $\sim$ 1 eV per H-atom more stable that their non-hydrogenated counterpart. Similar stabilization of ZnO systems after hydrogenation was observed in our previous work.[27]

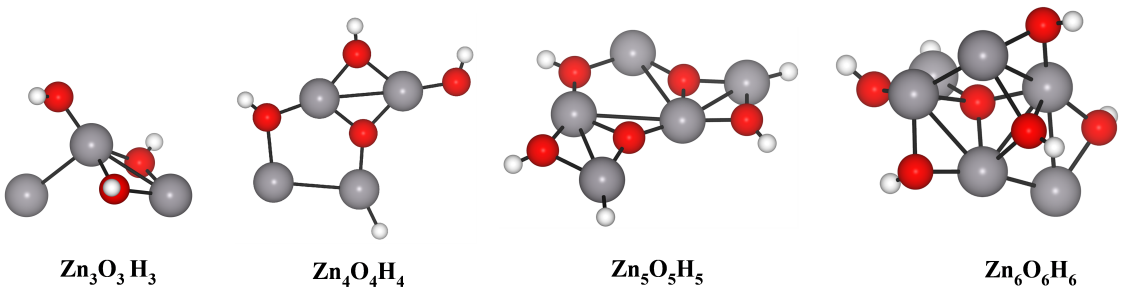

Figure 1: Effect of stoichiometric hydrogenation on ZnO clusters

To understand the chemical stability of the hydrogenated clusters we calculate the energy gap between the highest occupied molecular orbital (HOMO) and lowest unoccupied molecular orbital (LUMO). The HOMO-LUMO gaps of all the hydrogenated ZnO systems are tabulated in Table S3. We find that the HOMO-LUMO gap of all hydrogenated ZnO clusters decrease to 3-3.6 eV from the corresponding values 4-4.5 eV of the non-hydrogenated clusters. This indicates that the hydrogenated clusters are chemically more reactive and more polarizable than their non-hydrogenated counterparts. As a result, the hydrogenated clusters are expected to exhibit more chemical activity than the ZnO clusters.

Effect of hydroxylation of $(ZnOH)_n$ Clusters

During methanol synthesis from CO_2 the ZnO systems are exposed to hydrogen and water. In the previous subsection we discussed the effect of hydrogen incorporation on the structural and chemical properties of ZnO clusters. In this subsection, we will discuss the properties of the ZnO clusters in the presence of water molecules. It is reported that at the interface between ZnO-Cu of industrial catalyst water molecules gets splitted and OH species are generated.[7] These OH species can get adsorbed on the ZnO/Cu systems. Therefore, in this subsection, we will discuss the effect of incorporation of different concentration of OH species on the structural and chemical properties of ZnO clusters. The most stable ZnO clusters covered with OH species will be then placed on Cu(111) surface to understand the structure at the ZnO-Cu interface under methanol synthesis conditions. The global minima of the each of the ZnOH clusters covered with different amount of OH species are identified using the basin hopping method discussed in the section on Computational Details. The ZnO clusters with various concentration of OH are represented by $Zn_n(OH)_m$, where n=3 to 6 and m=n to 2n or greater than 2n. Note that m=n indicates the fully hydrogenated clusters.

Geometries of $Zn_n(OH)_m$ Clusters

We start our discussion with the hydroxylation of $(ZnOH)_3$ cluster. For this case in $(ZnOH)_3$ (where n=3) we systematically vary the amount of OH-ion (leading to m = 4, 5, 6, 7, 8) and locate the global minimum structures of $Zn_3(OH)_m$ clusters corresponding to each concentration (i.e, m) of OH. Note that the global minima obtained from basin hopping method are further optimised using Gaussian 09 program package as discussed in the computational details. The optimized geometries of $Zn_3(OH)_m$, m = 4, 5, 6, 7, 8, are given in Figure 2a. From this figure, we can see that the structures of $Zn_3(OH)_m$ clusters with 'm' up to 7 are comprised of a linear chain of three Zn-atoms connected with bridging OH group. The structure of $Zn_3(OH)_m$ cluster with m=8 tends to become angular again. To quantify the structural change occuring due to hydroxylation we analyse the bond lengths of different

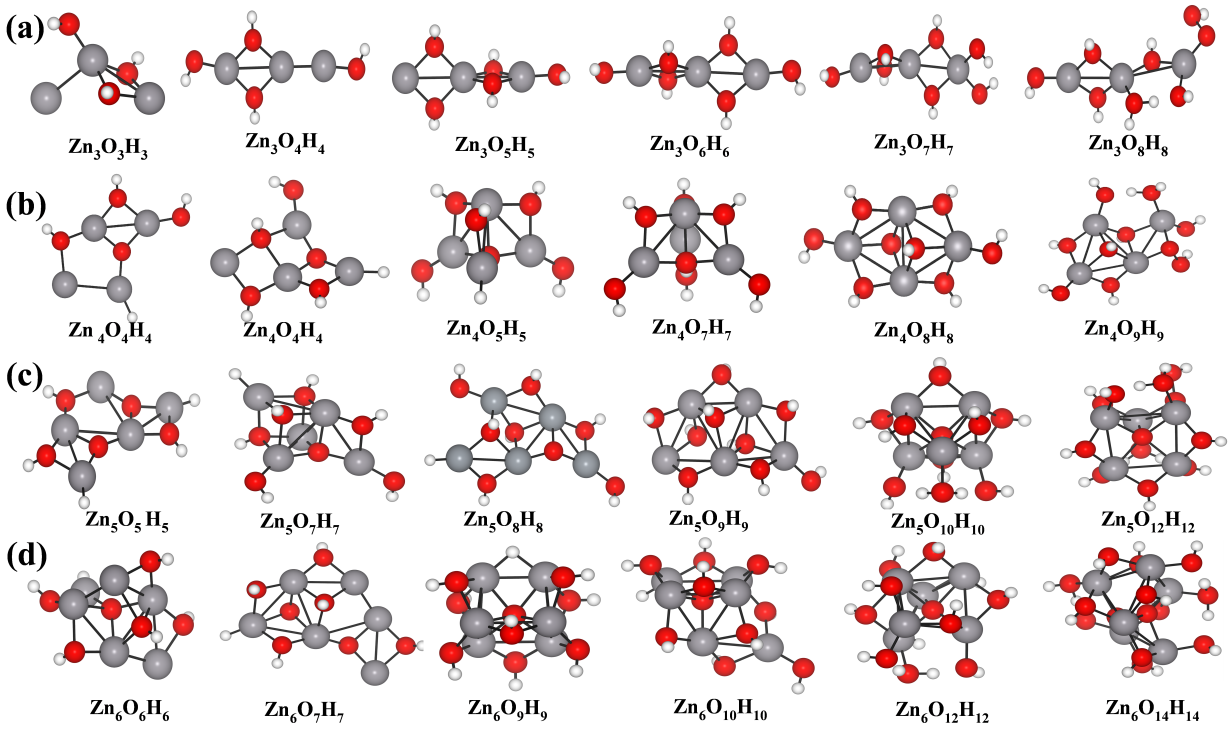

Figure 2: Global minima of (a) $Zn_3(OH)_m$, (b) $Zn_4(OH)_m$, (c) $Zn_5(OH)_m$, (d) $Zn_6(OH)_m$ clusters.

bonds formed in the clusters. We find that the first hydroxylation of the $(ZnOH)_3$ cluster results in shortening of the average Zn-Zn bond length to 2.77 Å from 3.23 Å in the $(ZnOH)_3$ cluster. Upon further addition of OH groups the average Zn-Zn bond length gets elongated and remains similar ($\sim$3 Å) for rest of the structures of $Zn_3(OH)_m$. Whereas, the average Zn-O bond lengths of all the hydroxylated $Zn_3(OH)_m$ clusters are found to 1.95 Å which is slightly smaller than the corresponding bond length in the hydrogenated $(ZnOH)_3$ clusters. For the case of n=4 we consider the values of m to be 5,6,9,8 and 10 and all the corresponding global minimum structures are obtained in the same manner as employed for the case of n=3. Unlike, the case of $Zn_3(OH)_m$ clusters the the hydroxylated clusters of $Zn_4(OH)_m$ series adopt quite different geometrical structures. In $Zn_4(OH)_5$ and $Zn_4(OH)_6$ we observe the formation of cage-like structure with an oxygen atom at the center. In particular, for the case of $Zn_4(OH)_6$ cluster a pyramidal structure is observed with 3 bridging OH groups, 2 terminal OH groups and 1 O atom being in the cage of 4 Zn atoms. In such

cage-like structures we also observe the formation of Zn-H bonds. Note that such systems with the capability of formation of hydride may be useful for the harvesting of hydrogen. The $Zn_4(OH)_8$ cluster adopts a bent hexagonal structure with 6 bridging OH and 2 terminal OH, whereas, $Zn_4(OH)_9$ and $Zn_4(OH)_{10}$ forms distorted structures from what is observed in $Zn_4(OH)_8$. Interestingly, we observe the formation of H_2O adsorbed to the clusters for cases beyond $Zn_4(OH)_8$. This indicates that cluster with four Zn-atoms can preferably accommodate 8 OH groups. The effect of adsorbed water on the stability of the cluster will be discussed later in this manuscript. In $Zn_4(OH)_6$ a shortening of the average Zn-Zn bond length(2.97 Å) is observed which then elongates (3.063 Å) in $Zn_4(OH)_8$. In $Zn_4(OH)_{10}$ Zn-Zn bond stretches further to 3.2 Å . Similar to Zn_3 series, upon H-addition the average Zn-O bond length increases from 1.79Å to 1.988Å which then remains the same through out the series. For $Zn_5(OH)_m$ series we consider OH groups with m=7,8,9,10,12. It is mentioned earlier that the $(ZnOH)_5$ shows a distorted planar structure with 3 bridged OH, two caged O among three Zn atoms and two H attached with terminal Zn atoms. Further hydroxylation of $(ZnOH)_5$ cluster gives rise to various interesting structures. For instance, $Zn_5(OH)_7$ shows a chair like structure, with 3 bridged OH groups, two caged O atoms among three Zn atoms, two terminal OH groups and one H atom attached with one Zn atom. Similarly, $Zn_5(OH)_8$ adopts a chair like structure with 6 bridged OH groups, one caged O, one terminal OH group and one H atom attached with Zn atom. Addition of one more OH group to this structure becomes $Zn_5(OH)_9$ which shows a structure similar to $Zn_5(OH)_5$ with 6 bridged OH groups, one terminal OH group and 2 OH groups bonded to three Zn atom each. Interestingly, $Zn_5(OH)_{10}$ adopts a crown like structure with 7 bridged OH groups, two terminal OH groups, one caged O atom among 4 Zn atoms and one water molecule attached to a Zn atom. Next member of this series, $Zn_6(OH)_{10}$ shows a distorted crown structure with an additional water molecule attached with Zn atom. The average Zn-Zn and Zn-O bond lengths of the $Zn_5(OH)_m$ clusters are elongated as compared to those of the $(ZnO)_5$ cluster due to the hydroxylation (see Table S1). Such bond elongation is also observed in the

previous clusters with n=3 and 5. However, the bond elongation is not uniform for all the members of $Zn_5(OH)_m$. For example, $Zn_5(OH)_9$ exhibits a Zn-Zn bond elongation of 0.33 Å as compared to its $(ZnO)_5$ values, whereas, $Zn_5(OH)_{10}$ shows a negligible elongation of 0.01 Å in the average Zn-Zn bond.

For $Zn_6(OH)_m$ series, m=7,8,9,10,12,14 are considered to study the effect of OH. The stable $(ZnOH)_6$ cluster with six member ring formed with Zn atoms and with bridged oxygens upon H addition attains a 3D structure with 5 bridging OH groups, one caged O and one H bonded with Zn atom. Further hydroxylation results in formation of $Zn_6(OH)_7$ which has some similarity with the zn5o7h7 and zn5o9h9. This cluster shows 4 bridged OH, two OH groups shared among three Zn atoms, one caged H and one H attached with a Zn atom. $Zn_6(OH)_9$ shows an inverted pyramidal structure with 8 bridging OH, one caged H and one bridged H. $Zn_6(OH)_{10}$ has some similarity with the previous cluster with some distortions and increased number of caged oxygens. $Zn_6(OH)_{12}$ shows more terminal OH groups and a water molecule attached to Zn atom. In $Zn_6(OH)_{14}$ we can observe one additional water compared to the previous cluster. The average Zn-Zn bond length has almost no change across the entire series. The average Zn-O bond length however increases slightly upon hydrogenation of $(ZnO)_6$ cluster, but, then remains more or less constant through out the series.

Electronic Properties of $Zn_n(OH)_m$ Clusters

To asses the stability of $Zn_n(OH)_m$ clusters with different concentration of OH groups we calculate the relative energies of the these clusters w.r.t. the $(ZnO)_n$ clusters using the relation

$$E_{rel}^{OH} = E_{Zn_n(OH)_m} - E_{(ZnO)_n} - (m-n)E_{OH} - nE_H \tag{2}$$

where, $E_{Zn_n(OH)_m}$ is the energy of the hydroxylated ZnO clusters and $E_{OH} = E_{H_2O} - \frac{1}{2}E_{H_2}$, E_{H_2O} is the energy of a H_2O molecule, $E_H = \frac{1}{2}E_{H_2}$, m indicates the amount of OH species

present in the system. Similar approach for calculating the stability of the hydroxylated ZnO systems was adopted in our previous work.[27] The relative energies of $Zn_n(OH)_m$ clusters are plotted in Figure 3 and the corresponding relative energy values are presented in Table S1 of the supplementary information. From Figure 3 we can see that for all the $Zn_n(OH)_m$ clusters

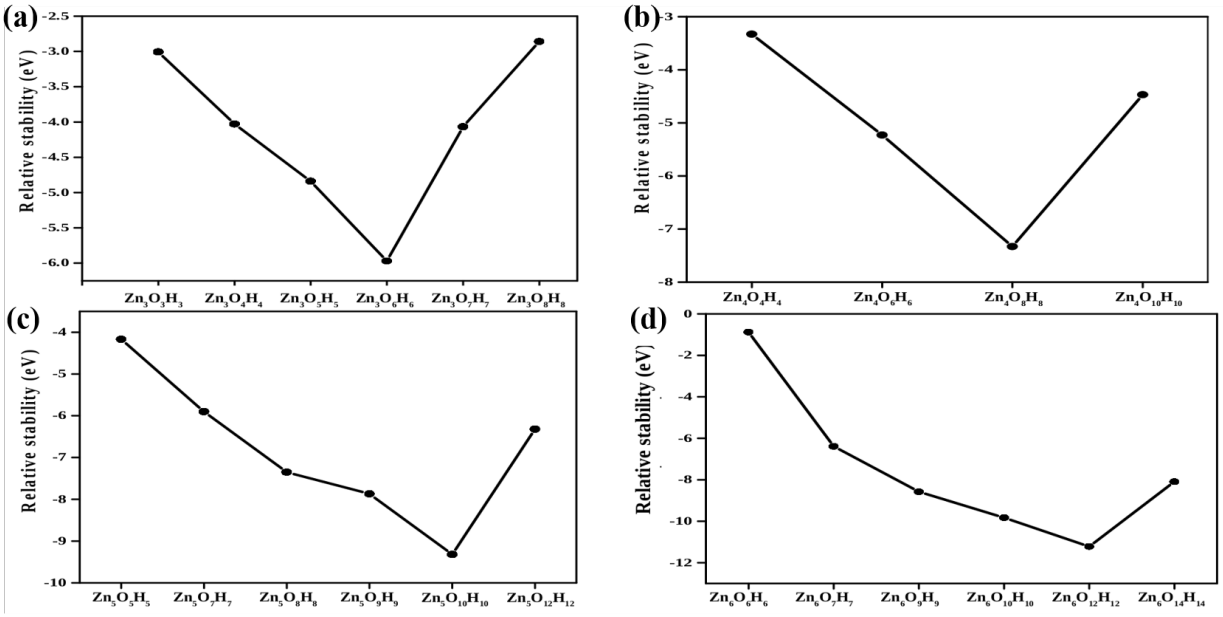

Figure 3: Plots of energies of (a) $Zn_3(OH)_m$, (b) $Zn_4(OH)_m$, (c) $Zn_5(OH)_m$, (d) $Zn_6(OH)_m$ clusters wrt their corresponding oxide clusters.

due to the addition of OH groups the stability increases almost linearly until the value of m=2n. Beyond this number (i.e, m > 2n) further hydroxylation decreases the stability of the clusters. This indicates that the cluster with n numbers of Zn-atoms can preferably accommodate 2n numbers of OH species which is similar to the ratio Zn:OH = 1:2 found in the bulk $Zn(OH)_2$ system.

The energy gap between highest occupied molecular orbital (HOMO) and lowest unoccupied molecular orbital (LUMO) of all the structures of $Zn_n(OH)_m$ are compiled in Table S1. From this table we can see that the HOMO-LUMO gap is highly dependent on the concentration of OH groups (values of m) present in the system. Interestingly, all the clusters with Zn:OH ratio of 1:2 shows similar energy gap of around 5.4 eV which is comparable to that of the bulk zinc hydroxide.[43] This high energy gap indicates that $Zn_n(OH)_m$ clusters with

n:m=1:2 are very stable systems. In Figure 4 we plot the molecular orbitals of HOMO and LUMO of different $Zn_n(OH)_m$ clusters with n:m=1:2. The molecular orbital plots show that

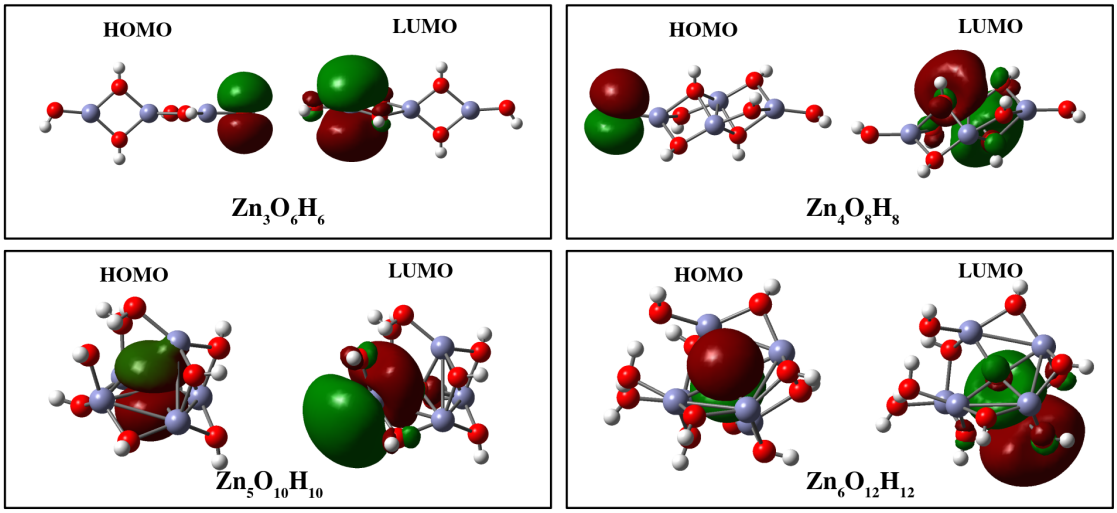

Figure 4: The plot of HOMO and LUMO of the most stable $Zn_n(OH)_m$ clusters

HOMO is mainly localized on OH for $Zn_3(OH)_6$ and $Zn_4(OH)_8$ clusters whereas, the same is mostly localised on caged O-atom of $Zn_5(OH)_{10}$ and $Zn_6(OH)_{12}$ clusters. On the other hand, LUMO is mostly centred around Zn-atom of the $Zn_n(OH)_m$ clusters with n:m=1:2 clusters considered in the present work. From the Figure 4 it is very clear that for the smaller systems where n=3 and 4 the HOMO and LUMO are spatially well separated in the space. This indicates that the $Zn_3(OH)_6$ and $Zn_4(OH)_8$ clusters may exhibit good optical response for applications in optoelectronics.

The infra-red (IR) spectrum of the most stable clusters are shown in Figure 5. These spectra clearly capture the presence of water on the surfaces of $Zn_5(OH)_{10}$ and $Zn_6(OH)_{12}$ as the significant peaks at 3000 cm^{-1}. The presence of terminal OH groups is observed near 4000 cm^{-1}. Here, we wish to highlight that the peak intensity of the terminal OH decreases with increasing size of the cluster, which indicates the formation of cage like structure in the cases of bigger clusters. After the discussion on the structural and electronic properties of hydoxylated ZnO clusters in the gas phase, we next proceed to investigate the chemical reactivity towards CO_2 molecule.

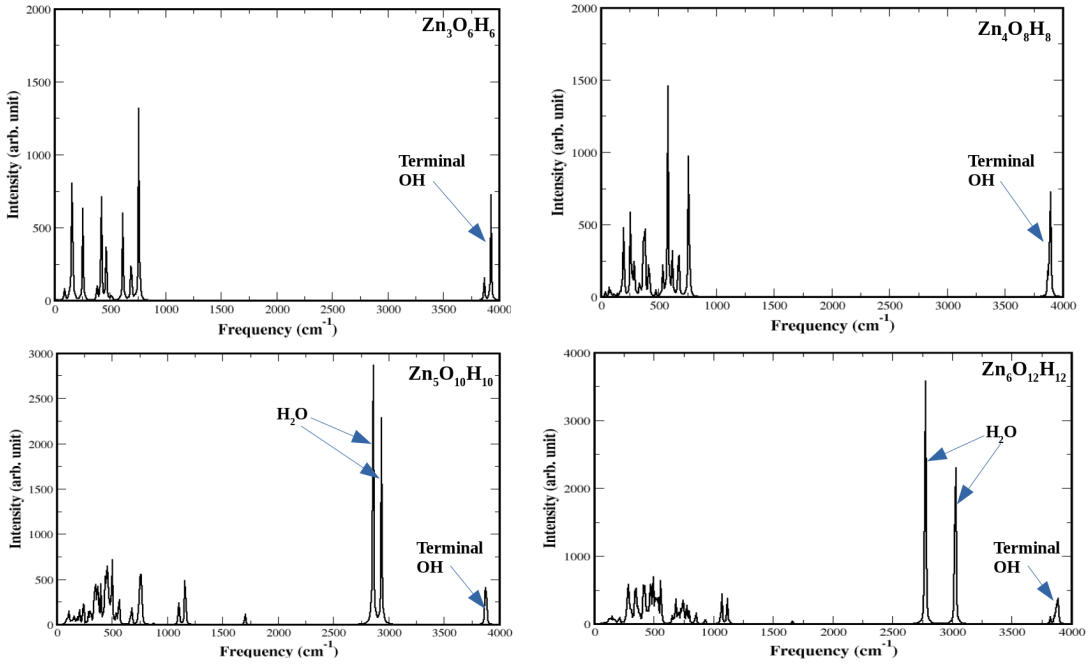

Figure 5: Infra-Red spectra of the most stable clusters of $Zn_n(OH)_m$

Structural Properties of $Zn_n(OH)_m$ Clusters Supported on Cu(111) surface

To understand the effect of Cu surface on the structural and chemical properties of $Zn_n(OH)_m$ Clusters we re-optimize the geometries of the most stable candidates (i.e.$Zn_3(OH)_6$, $Zn_4(OH)_8$, $Zn_5(OH)_{10}$ and $Zn_6(OH)_{12}$) placing them on Cu(111) surface. The optimized geometries of the most stable candidates of $Zn_n(OH)_m$ supported on Cu(111) are given in Figure 6. Compared to the gas phase structure, $Zn_3(OH)_6$ shows slight shortening of average Zn-Zn bond length upon deposition on Cu surface. Slight increase in Zn-Zn bond length is observed for $Zn_5(OH)_{10}$. The remaining two clusters do not undergo any significant structural change when they are deposited on Cu surface. The average Zn-O bond length remains almost same for all of the four clusters. The interaction between the clusters and the Cu surface is estimated through the calculation of adsorption energy using the following equation,

$$E_{ads} = E_{Zn_n(OH)_m - Cu(111)} - E_{Zn_n(OH)_m} - E_{Cu(111)} \tag{3}$$

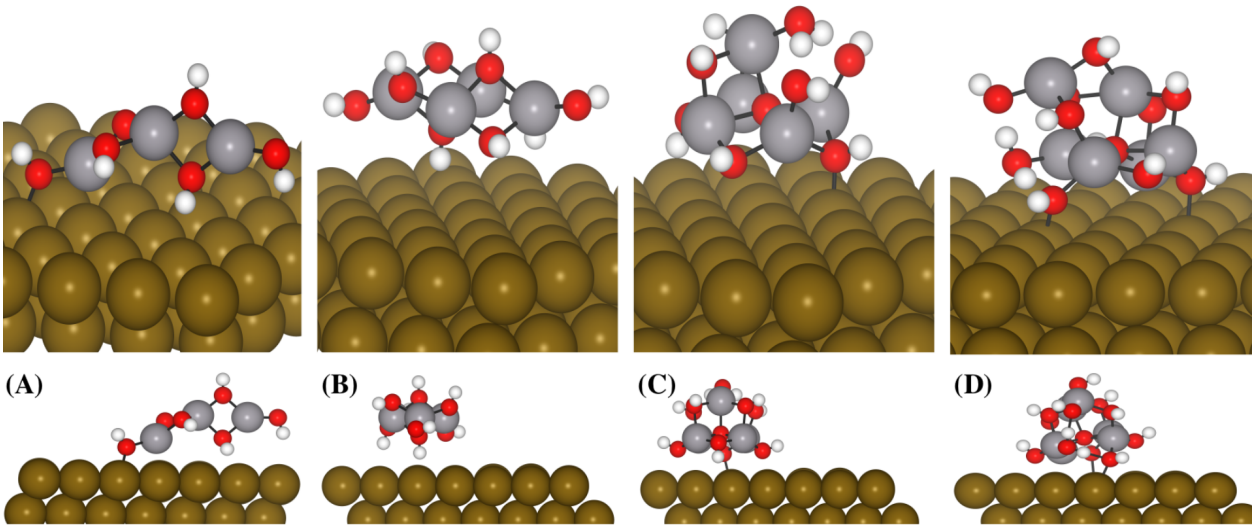

Figure 6: Geometries of the most stable candidates of $Zn_n(OH)_m$ supported on Cu(111); A,$Zn_3(OH)_6$; B,$Zn_4(OH)_8$; C,$Zn_5(OH)_{10}$, D,$Zn_6(OH)_{12}$

Where, E_{ads} is the adsorption energy, $E_{Zn_n(OH)_m-Cu(111)}$ is the energy of the cluster on the CU(111) surface, $E_{Zn_n(OH)_m}$ is the energy of the cluster in the gasphase, $E_{Cu(111)}$ is the energy of the pure Cu(111) surface. The adsorption energies of these clusters on Cu(111) surface are tabulated in Table S2. From this table we find that the larger clusters i.e, $Zn_5(OH)_{10}$ and $Zn_6(OH)_{12}$ exhibit stronger interaction with the surface as compared to that of the smaller ($Zn_3(OH)_6$ and $Zn_4()H)_8$) clusters. In particular, $Zn_4(OH)_8$ shows the least interaction with the Cu surface due to its very symmetrical and stable structure.

Interaction of CO_2 with Free and Cu(111) Supported $Zn_n(OH)_m$ Systems

To investigate the chemical reactivity of $Zn_n(OH)_m$ clusters towards CO_2, we allow a CO_2 molecule to get adsorbed on various sites of $Zn_n(OH)_m$ clusters. The strength of the interaction between the CO_2 molecule and the cluster is estimated by calculating the adsorption

energy using the formula,

$$E_{ads} = E_{system-CO_2} - E_{system} - E_{CO_2} \tag{4}$$

where, E_{ads} is the adsorption energy, $E_{system-CO_2}$ is the energy of the CO_2 adsorbed system, E_{system} is the energy of the optimized system, E_{CO_2} is the energy of the CO_2 molecule in gas phase. We find that the CO_2 preferably gets adsorbed on the Zn-site of the clusters. The adsorption energies of CO_2 on selected $Zn_n(OH)_m$ clusters are compiled in Table 1. From this table it can be seen that the adsorption energy of CO_2 on $Zn_n(OH)_m$ clusters lies in the range - 0.1 to -0.2 eV and the change in O-C-O bond angle of the adsorbed CO_2 as compared to its linear form is also found to be negligible. This clearly indicates that all the $Zn_n(OH)_m$ clusters including the hydrogenated ones (where n=m) interact very weakly with CO_2 molecule. In particular, we observe that the larger clusters like $Zn_5(OH)_m$ or $Zn_6(OH)_m$

Table 1: Adsorption energy (E_{ads}) of CO_2 and the change in O-C-O bond angle of CO_2 ($\Delta\angle$O-C-O) when it gets adsorbed on $Zn_n(OH)_m$ clusters

System	Adsorption Energy(eV)	$\Delta\angle$O-C-O
$Zn_3(OH)_3$	-0.17	2.2
$Zn_3(OH)_6$	-0.19	4.2
$Zn_3(OH)_6$/Cu(111)	-0.24	1.0
$Zn_3(OH)_8$	-0.19	4.2
$Zn_4(OH)_4$	-0.14	1.6
$Zn_4(OH)_8$	-0.09	1.5
$Zn_4(OH)_8$/Cu(111)	-0.17	1.7
$Zn_4(OH)_{10}$	-0.23	5.4
$Zn_5(OH)_5$	-0.08	1.7
$Zn_5(OH)_{10}$	-0.07	2.0
$Zn_5(OH)_{10}$/Cu(111)	-0.20	0.9
$Zn_5(OH)_{12}$	-0.09	5.4
$Zn_6(OH)_6$	-0.09	0.6
$Zn_6(OH)_{12}$	-0.09	1.1
$Zn_6(OH)_{12}$/Cu(111)	-0.15	1.0
$Zn_6(OH)_{14}$	-0.09	1.1

exhibit more weaker interaction as compared to that of $Zn_3(OH)_m$ or $Zn_4(OH)_m$. This is because of the non-availability of the open Zn-sites in the cage-like geometries of the bigger clusters. The adsorbed H_2O molecule on the Zn-sites of these clusters can be attributed for the blocking of the Zn-site. We find that the adsorption energy of such water molecule on these clusters is $\sim$ -0.4 eV indicating a possibility of the removal of this water molecule at room temperature with the help of entropic energy. Therefore, we also calculate the adsorption energy of CO_2 on the bigger clusters ($Zn_5(OH)_m$ or $Zn_6(OH)_m$) after removing the adsorbed H_2O. We observe that the bigger clusters without H_2O show more reactivity towards CO_2 by $\sim$ 0.05 eV as compared to their corresponding with H_2O cases. Therefore, it is evident that water may block the reaction centre in ZnO systems for the adsorption of CO_2 and thereby hindering the subsequent hydrogenation process. Here, we wish to mention that the effect of water poisoning of ZnO/Cu systems during methanol synthesis is experimentally observed in the previous literature.[44,45]

After the discussion on adsorption and activation of CO_2 on free $Zn_n(OH)_m$ clusters, we proceed further to understand the effect of Cu surface on this reaction. To this end, we first deposit the most stable clusters of $Zn_n(OH)_m$ on Cu(111) surface and the adsorption and activation of CO_2 is investigated at the $Zn_n(OH)_m$-Cu(111) interface. Note that [111] plane is reported to be the most stable surface of Cu, therefore, this surface is widely used for the investigation of methanol synthesis on ZnO/Cu systems.[5,6,18,26,27] The details of the structure of $Zn_n(OH)_m$/Cu(111) systems are discussed in the supplementary information. We find that all the $Zn_n(OH)_m$ clusters weakly interact with the surface. However, the details of structural evolution of $Zn_n(OH)_m$ clusters on Cu surface under realistic reaction conditions is deferred for the future work. The adsorption energies of CO_2 on $Zn_n(OH)_m$/Cu(111) systems for the cases of $Zn_3(OH)_6$, $Zn_4(OH)_8$, $Zn_5(OH)_{10}$ and $Zn_6(OH)_{12}$ clusters are given in Table 1. From this table we find that the adsorption of CO_2 on $Zn_n(OH)_m$/Cu(111) systems is slightly higher by $\sim$0.05 eV than that of the corresponding gas phase values. However, the adsorption of CO_2 on $Zn_n(OH)_m$/Cu(111) systems is still found to be very weak. Such weak

interaction between ZnO clusters and CO_2 is also reported in the literature.[26]

Conclusion

In summary, we investigate the structural and chemical properties of free and Cu(111) supported $(ZnO)_n$, where n=3-6, nanoclusters in presence of hydrogen and water. It is observed that the ring-like structures of pure ZnO clusters in the gas phase alter drastically upon hydrogenation. In particular, the bigger clusters like $Zn_6(OH)_6$ adopt a cage-like structure, whereas, the pure $(ZnO)_6$ cluster shows a pentagonal ring with sides constructed by O-Zn-O. Further, we investigate the structural and stoichiometry evolution of ZnO clusters in the presence of water. We find that the stability of the ZnO clusters increases with the concentration of OH species which is derived from water molecules. Interestingly, we observe that all the ZnO clusters attain a maximum stability of $\sim$ -1.9 eV per Zn atom, relative to their corresponding pure phases, when the ratio between Zn and OH in the system is 1:2, which is similar to that observed in the case of bulk phase of $Zn(OH)_2$. The amount of OH beyond twice of Zn-atoms leads to the decrease in the stability of the system. Moreover, we observe that the ZnO clusters with Zn:OH=1:2 show very large energy gap of $\sim$5 eV between the HOMO and LUMO which is comparable to the band gap of bulk $Zn(OH)_2$. It is very clear from our study that variously hydroxylated ZnO clusters are much more stable in the presence of water and hydrogen than the original ZnO clusters. Importantly, we also predict a structural transition for the most stable $Zn_m(OH)_2m$ clusters from planar 2D configurations up to size $m = 4$ to 3D configurations for larger sizes, a transition associated with the disproportionation of two hydroxyl units into an oxygen atom buried in the cluster core plus a water molecule adsorbed on the cluster surface. This might also be of general significance, and may possibly suggest the formation for larger systems of ZnO bulk coated with a $Zn(OH)_2$ shell. Moreover, we find that the $Zn_m(OH)_2m$ clusters are also stabilized under methanol synthesis conditions (temperature = 500K, 1 bar of H_2O and 40 bar of H_2

partial pressures). Further, we investigate the chemical properties of these ZnO clusters towards adsorption and activation of CO_2. It is observed that all the clusters exhibit very weak interaction (E_{ads} is -0.1 to -0.2 eV) with CO_2. For the cases of bigger clusters we observe the effect of water poisoning leading to the hindrance to adsorption of CO_2. Finally, we highlight the role of the Cu surface, which is used to support the ZnO clusters, for the adsorption of CO_2. It is observed that the $Zn_n(OH)_m$/Cu(111) systems are slightly more active towards the adsorption of CO_2 than that of the free $Zn_n(OH)_m$ clusters. However, all the systems studied in the present work exhibit negligible activation of CO_2, which is consistent with previous reports on ZnO/Cu systems.[26] Therefore, we infer that the systems reported here may show similar catalytic activities of the reported ZnO/Cu systems for the hydrogenation of CO_2 towards methanol.

Acknowledgement

KM and SD acknowledges the support and the resources provided by 'PARAM Shivay Facility' under the National Supercomputing Mission, Government of India at the Indian Institute of Technology, Varanasi. KM also acknowledges the Department of Science and Technology, Government of India, for funding (DST/INSPIRE/04/2018/002482).

Supporting Information Available

Computational methodology, Table S1 : Structural evolution of clusters upon H and OH addition and Structural analysis, Table S2: Comparison of Zn-O bonds in our calculation vs literature, Table S3 :Effect of hydrogenation on ZnO Clusters,Table S4: Effect of temperature and pressure on relative stability of per Zn atom of clusters, Table S5: Effect of Cu surface on most stable clusters, , Table S6 and S7: Comparison of CO_2 adsorption energy of clusters in different environment, Table S8: Comparison of CO_2 adsorption energy of clusters with van der waals correction (DFT-D3), Table s9: Comparison of CO_2 adsorption energy of clusters

deposited on Cu surface with van der waals correction(TS-09)

References

(1) Sun, X. W.; Huang, J. Z.; Wang, J. X.; Xu, Z. A ZnO Nanorod Inorganic/Organic Heterostructure Light-Emitting Diode Emitting at 342 nm. *Nano Lett.* **2008**, *8*, 1219–1223.

(2) Cao, X.; Wang, N.; Wang, L. Ultrathin ZnO Nanorods: Facile Synthesis, Characterization and Optical Properties. *Nanotechnology* **2010**, *21*, 065603.

(3) Jang, E.; Won, J.-H.; Hwang, S.-J.; Choy, J.-H. Fine Tuning of the Face Orientation of ZnO Crystals to Optimize Their Photocatalytic Activity. *Adv. Mater.* **2006**, *18*, 3309–3312.

(4) Fortunato, E.; Barquinha, P.; Martins, R. Oxide Semiconductor Thin-Film Transistors: A Review of Recent Advances. *Adv. Mater.* **2012**, *24*, 2945–2986.

(5) Behrens, M.; Studt, F.; Kasatkin, I.; Kühl, S.; Hävecker, M.; Abild-Pedersen, F.; Zander, S.; Girgsdies, F.; Kurr, P.; Kniep, B.-L.; et al, The Active Site of Methanol Synthesis over $Cu/ZnO/Al_2O_3$ Industrial Catalysts. *Science* **2012**, *336*, 893–897.

(6) Kattel, S.; Ramírez, P. J.; Chen, J. G.; Rodriguez, J. A.; Liu, P. Active Sites for CO_2 Hydrogenation to Methanol on Cu/ZnO Catalysts. *Science* **2017**, *355*, 1296–1299.

(7) Zhang, Z.; Chen, X.; Kang, J.; Yu, Z.; Tian, J.; Gong, Z.; Jia, A.; You, R.; Qian, K.; He, S.; et al, The Active Sites of Cu–ZnO Catalysts for Water Gas Shift and CO Hydrogenation Reactions. *Nat. Commun.* **2021**, *12*, 4331.

(8) Mora-Fonz, D.; Lazauskas, T.; Farrow, M. R.; Catlow, C. R. A.; Woodley, S. M.; Sokol, A. A. Why Are Polar Surfaces of ZnO Stable? *Chem. Mat.* **2017**, *29*, 5306–5320.

(9) Mora-Fonz, D.; Buckeridge, J.; Logsdail, A. J.; Scanlon, D. O.; Sokol, A. A.; Woodley, S.; Catlow, C. R. A. Morphological Features and Band Bending at Nonpolar Surfaces of ZnO. *J. Phys. Chem. C* **2015**, *119*, 11598–11611.

(10) Johar, M. A.; Afzal, R. A.; Alazba, A. A.; Manzoor, U. Photocatalysis and bandgap engineering using ZnO nanocomposites. *Advances in Materials Science and Engineering* **2015**, *2015*.

(11) Lee, K. M.; Lai, C. W.; Ngai, K. S.; Juan, J. C. Recent developments of zinc oxide based photocatalyst in water treatment technology: a review. *Water research* **2016**, *88*, 428–448.

(12) Kumar, S. G.; Rao, K. K. Zinc oxide based photocatalysis: tailoring surface-bulk structure and related interfacial charge carrier dynamics for better environmental applications. *Rsc Advances* **2015**, *5*, 3306–3351.

(13) Kulmas, M.; Paterson, L.; Höflich, K.; Bashouti, M. Y.; Wu, Y.; Göbelt, M.; Ristein, J.; Bachmann, J.; Meyer, B.; Christiansen, S. Composite nanostructures of TiO2 and ZnO for water splitting application: Atomic layer deposition growth and density functional theory investigation. *Advanced Functional Materials* **2016**, *26*, 4882–4889.

(14) Sudha, D.; Sivakumar, P. Review on the photocatalytic activity of various composite catalysts. *Chemical Engineering and Processing: Process Intensification* **2015**, *97*, 112–133.

(15) Zhang, Y.; Ram, M. K.; Stefanakos, E. K.; Goswami, D. Y. Synthesis, characterization, and applications of ZnO nanowires. *Journal of Nanomaterials* **2012**, *2012*.

(16) Lunkenbein, T.; Schumann, J.; Behrens, M.; Schlögl, R.; Willinger, M. G. Formation of a ZnO Overlayer in Industrial $Cu/ZnO/Al_2O_3$ Catalysts Induced by Strong Metal-Support Interactions. *Angew. Chem. Int. Ed.* **2015**, *54*, 4544–4548.

(17) Kuld, S.; Thorhauge, M.; Falsig, H.; Elkjær, C. F.; Helveg, S.; Chorkendorff, I.; Sehested, J. Quantifying the Promotion of Cu Catalysts by ZnO for Methanol Synthesis. *Science* **2016**, *352*, 969–974.

(18) Senanayake, S. D.; Ramírez, P. J.; Waluyo, I.; Kundu, S.; Mudiyanselage, K.; Liu, Z.; Liu, Z.; Axnanda, S.; Stacchiola, D. J.; Evans, J.; et al, Hydrogenation of CO_2 to Methanol on CeO_x/Cu(111) and ZnO/Cu(111) Catalysts: Role of the Metal-Oxide Interface and Importance of Ce^{3+} Sites. *J. Phys. Chem. C* **2016**, *120*, 1778–1784.

(19) Waugh, K. C. Methanol Synthesis. *Catal. Lett.* **2012**, *142*, 1153–1166.

(20) Saedy, S.; Newton, M. A.; Zabilskiy, M.; Lee, J. H.; Krumeich, F.; Ranocchiari, M.; van Bokhoven, J. A. Copper–zinc oxide interface as a methanol-selective structure in Cu–ZnO catalyst during catalytic hydrogenation of carbon dioxide to methanol. *Catal. Sci. Technol.* **2022**, *12*, 2703–2716.

(21) Jiang, F.; Yang, Y.; Wang, L.; Li, Y.; Fang, Z.; Xu, Y.; Liu, B.; Liu, X. Dependence of copper particle size and interface on methanol and CO formation in CO2 hydrogenation over Cu@ZnO catalysts. *Catal. Sci. Technol.* **2022**, *12*, 551–564.

(22) Koplitz, L. V.; Dulub, O.; Diebold, U. STM Study of Copper Growth on ZnO(0001)-Zn and ZnO(000$\bar{1}$)-O Surfaces. *J. Phys. Chem. B* **2003**, *107*, 10583–10590.

(23) Dulub, O.; Batzill, M.; Diebold, U. Growth of Copper on Single Crystalline ZnO: Surface Study of a Model Catalyst. *Top. Catal.* **2005**, *36*, 65–76.

(24) Paleico, M. L.; Behler, J. Global Optimization of Copper Clusters at the ZnO(101$\bar{0}$) Surface using a DFT-based Neural Network Potential and Genetic Algorithms. *J. Chem. Phys.* **2020**, *153*, 054704.

(25) Higham, M. D.; Mora-Fonz, D.; Sokol, A. A.; Woodley, S. M.; Catlow, C. R. A. Mor-

phology of Cu Clusters Supported on Reconstructed Polar ZnO (0001) and (000$\bar{1}$) Surfaces. *J. Mater. Chem. A* **2020**, *8*, 22840–22857.

(26) Reichenbach, T.; Mondal, K.; Jäger, M.; Vent-Schmidt, T.; Himmel, D.; Dybbert, V.; Bruix, A.; Krossing, I.; Walter, M.; Moseler, M. Ab initio Study of CO_2 Hydrogenation Mechanisms on Inverse ZnO/Cu Catalysts. *J. Catal.* **2018**, *360*, 168–174.

(27) Mondal, K.; Sharma, M.; Banerjee, A.; Fortunelli, A.; Walter, M.; Moseler, M. Ab Initio Modeling of the ZnO-Cu(111) Interface. *The Journal of Physical Chemistry C* **2021**, *126*.

(28) Reichenbach, T.; Walter, M.; Moseler, M.; Hammer, B.; Bruix, A. Effects of Gas-Phase Conditions and Particle Size on the Properties of Cu(111)-Supported Zn_yO_x Particles Revealed by Global Optimization and Ab Initio Thermodynamics. *J. Phys. Chem. C* **2019**, *123*, 30903–30916.

(29) Wu, J.; Saito, M.; Takeuchi, M.; Watanabe, T. The stability of Cu/ZnO-based catalysts in methanol synthesis from a CO2-rich feed and from a CO-rich feed. *Applied Catalysis A: General* **2001**, *218*, 235–240.

(30) Athanasios Zachopoulosa, E. H. Overcoming the equilibrium barriers of CO2 hydrogenation to methanol via water sorption: A thermodynamic analysis. *Journal of CO2 Utilization* **2017**, *21*, 360–367.

(31) Szakacs, C.; Merschrod, E.; Poduska, K. Structural Features That Stabilize ZnO Clusters: An Electronic Structure Approach. *Computation* **2013**, *1*, 16–26.

(32) Wang, B.; Wang, X.; Chen, G.; Nagase, S.; Zhao, J. Cage and tube structures of medium-sized zinc oxide clusters (ZnO)n (n=24, 28, 36, and 48). *The Journal of Chemical Physics* **2008**, *128*, 144710.

(33) Wang, B.; Nagase, S.; Zhao, J.; Wang, G. Structural Growth Sequences and Electronic Properties of Zinc Oxide Clusters (ZnO)n (n=2-18). *Journal of Physical Chemistry C - J PHYS CHEM C* **2007**, *111*.

(34) Mortensen, J. J.; Hansen, L. B.; Jacobsen, K. W. Real-space grid implementation of the projector augmented wave method. *Phys. Rev. B* **2005**, *71*, 035109.

(35) Enkovaara, J. et al. Electronic structure calculations with GPAW: a real-space implementation of the projector augmented-wave method. *Journal of Physics: Condensed Matter* **2010**, *22*, 253202.

(36) Wales, D. J.; Doye, J. P. K. Global Optimization by Basin-Hopping and the Lowest Energy Structures of Lennard-Jones Clusters Containing up to 110 Atoms. *The Journal of Physical Chemistry A* **1997**, *101*, 5111–5116.

(37) Rondina, G. G.; Da Silva, J. L. F. Revised Basin-Hopping Monte Carlo Algorithm for Structure Optimization of Clusters and Nanoparticles. *Journal of Chemical Information and Modeling* **2013**, *53*, 2282–2298, PMID: 23957311.

(38) Becke, A. D. Density-functional exchange-energy approximation with correct asymptotic behavior. *Phys. Rev. A* **1988**, *38*, 3098–3100.

(39) Hay, P. J.; Wadt, W. R. Ab initio effective core potentials for molecular calculations. Potentials for the transition metal atoms Sc to Hg. *The Journal of Chemical Physics* **1985**, *82*, 270–283.

(40) Kendall, R. A.; Dunning, T. H.; Harrison, R. J. Electron affinities of the first-row atoms revisited. Systematic basis sets and wave functions. *The Journal of Chemical Physics* **1992**, *96*, 6796–6806.

(41) Perdew, J. P.; Burke, K.; Ernzerhof, M. Generalized Gradient Approximation Made Simple. *Phys. Rev. Lett.* **1996**, *77*, 3865–3868.

(42) Bitzek, E.; Koskinen, P.; Gähler, F.; Moseler, M.; Gumbsch, P. Structural Relaxation Made Simple. *Physical review letters* **2006**, *97*, 170201.

(43) Wang, M.; Jiang, L.; Kim, E. J.; Hahn, S. H. Electronic structure and optical properties of Zn(OH)2: LDA+U calculations and intense yellow luminescence. *RSC Adv.* **2015**, *5*, 87496–87503.

(44) Prašnikar, A.; Likozar, B. Sulphur poisoning, water vapour and nitrogen dilution effects on copper-based catalyst dynamics, stability and deactivation during CO2 reduction reactions to methanol. *React. Chem. Eng.* **2022**, *7*, 1073–1082.

(45) Samimi, F.; Rahimpour, M. R.; Shariati, A. Development of an Efficient Methanol Production Process for Direct CO2 Hydrogenation over a Cu/ZnO/Al2O3 Catalyst. *Catalysts* **2017**, *7*.